UNIVERSITÀ DEGLI STUDI DI TORINO

Translocation of the proto-oncogene Bcl-6 in human glioblastoma multiforme

Simona Raggiera1, Roberto Tamma1, Andrea Marzullo[2], Tiziana Annese[1], Christian Marinaccio[1], Mariella Errede[1], Francesco C. Susca[3], Rebecca Senetta[4], Paola Cassoni[4], Angelo Vacca[3], Francesco Albano[5], Chiara Saracino[6], Angelo Notarangelo[6], Giorgina Specchia[5], Domenico Ribatti[1, 7], Beatrice Nico[1]

[1] Department of Basic Medical Sciences, Neurosciences and Sensory Organs, University of Bari Medical School, Bari, Italy

[2] Department of Emergency and Transplantation, Pathology Unit, University of Bari Medical School, Bari, Italy

[3] Department of Internal Medicine and Clinical Oncology, University of Bari Medical School, Bari, Italy

[4] Department of Medical Sciences, University of Turin Medical School, Turin, Italy

[5] Department of Emergency and Transplantation, Hematology Unit, University of Bari Medical School, Bari, Italy

[6] Medical Genetics Unit, IRCCS Casa Sollievo della Sofferenza Hospital, San Giovanni Rotondo (FG), Italy

[7] National Cancer Institute "Giovanni Paolo II", Bari, Italy

Highlights

The role of Bcl-6 translocation in cerebral tumors is unclear.
We have investigated Bcl-6 translocation in GBM, low-grade glioma, and meningioma.
We have demonstrated that the Bcl-6 translocates in GBM.
Translocation correlates with apoptosis inhibition, indicating a key role in GBM.

Abstract

Bcl-6 translocation is a genetic alteration that is commonly detected in Primary Central Nervous System Lymphoma. The role of this protein in cerebral tumors is unclear. In this study we investigated Bcl-6 translocation and its transcriptional and translational levels in formalin-fixed, paraffin-embedded cerebral tissue sections from glioblastoma (GBM), low-grade glioma (Astrocytoma grade II and III), and meningioma patients, and correlated them with apoptotic processes and p53 and caspase-3 expression. The results showed a frequency of 36.6% of Bcl-6 translocation in GBM patients and a decreased expression in low-grade glioma patients, correlated with the severity of the disease. Bcl-6 translocation induced an overexpression of both Bcl-6 protein and messenger in GBM, inhibiting apoptotic processes and caspases 3 expression. On the contrary, in low-grade gliomas and meningiomas Bcl-6 expression was reduced, resulting in an increase of apoptotic processes. Finally, p53 expression levels in brain tumors were comparable to Bcl-6 levels. Overall, these data demonstrate, for the first time, that the Bcl-6 gene translocates in GBM patients and that its translocation and expression are correlated with apoptosis inhibition, indicating a key role for this gene in the control of cellular proliferation. This study offers further insights into glioblastoma biology, and supports Bcl-6 as a new diagnostic marker to evaluate the disease severity.

Keywords

Brain tumors; Bcl-6; Glioma; Tumor progression

2

Introduction

Glioblastoma (GBM) multiforme is one of the most common and aggressive primary brain tumors in adults. It is characterized by rapid proliferation, diffuse invasion, necrosis, high angiogenesis and resistance to treatment. Median survival ranges from 9 to 12 months[1] and[2]. Malignant gliomas are classified on the basis of their histopathological features and their degree of malignancy, as diffuse astrocytoma, grade II; anaplastic astrocytoma, grade III; and glioblastoma, grade IV[3] . A distinction can also be made between secondary glioblastomas developing from pre-existing grade III gliomas, and *de novo* primary glioblastomas.

In gliomas, many genetic alterations, such as TP53 mutations, epidermal growth factor receptor (EGFR) amplification, p16INK4a homozygous deletion, phosphatase and tensin[4] homolog (PTEN) mutations, loss of heterozygosity (LOH) 10q, LOH 1p, and LOH 19q and[5], are recognizable, leading to the activation of oncogenes and inactivation of tumor suppressor genes. These genetic alterations interfere with critical cell cycle points, growth factor activation, apoptosis, cell motility and invasion pathways, and are responsible for phenotypic changes and neoplastic transformation[6]. Recently, somatic mutations of $NADP^+$-dependent isocitrate dehydrogenase 1 (IDH1)[7], now considered to be a highly selective molecular marker of GBMs[8], have been identified. IDH1 mutations confer a new enzymatic function to this protein, leading to a potential indirect promotion of angiogenesis in glioma, and could also influence epigenetic regulation, suggesting an early role in glioma tumorigenesis[9]. Therefore, IDH1 mutations are more frequent in secondary GBMs and are often associated with TP53 mutations and LOH 19q, whereas GBMs without IDH1 mutations often show EGFR amplification[8].

B-cell lymphoma 6 (Bcl-6) is a proto-oncogene located on chromosome 3 band q27 encoding a nuclear sequence-specific transcriptional repressor of 706 amino acids with a molecular weight of 78,846 Da. In normal conditions, Bcl-6 regulates germinal center (GC) formation and plays a central role in the regulation of B and T cell development, modulating the transcription of genes involved in cell proliferation, differentiation and apoptosis[10],[11]and [12]. By contrast, Bcl-6 is not expressed in other districts because its promoter is silent[13].

The breakpoints of Bcl-6 translocations are mainly clustered at the 5′ non-coding regulatory region, so Bcl-6 expression becomes deregulated by translocations in which heterologous promoters/enhancers replace normal Bcl-6 regulatory sequences [14] and [15].

A translocation of Bcl-6 has been demonstrated in 20–40% of Primary Lymphomas of the Central Nervous System (PCNLS)[16] and in a variety of lymphoid malignancies such as large B cell Lymphomas[17],[18] and [19]. In lymphoma, several reports in literature have analyzed patients survival in terms of the incidence and a favorable[20] and [21] or unfavorable prognosis[17] of the Bcl-6 rearrangement. The biological significance of Bcl-6 in GBM has not yet been elucidated and no evidence of genetic mutations involving the Bcl6 gene has yet been reported.

The purpose of this study was to analyze Bcl-6 gene expression, its protein and messenger content on biopsy specimens obtained from different groups of patients, affected by GBM, astrocytoma grade II/III, and low index of malignancy meningioma, using healthy human brain specimens as negative, and PCNLS as positive controls. FISH, immunohistochemistry with related densitometrical analysis, and Real Time PCR were performed. Moreover, because Bcl-6 is a transcriptional repressor of the genes involved in apoptosis, we correlated translocation of the Bcl6 gene with the degree of tumor aggressiveness and with the regulation of apoptotic processes, by Tunel assay, and with p53 and caspase-3 immunocytochemical expression, in all groups of samples.

The results demonstrate, for the first time, a frequency of 36.6% of Bcl-6 translocation in GBM patients, and a progressive translocation decrease in other gliomas, paralleling the tumor aggressiveness. Moreover, both Bcl-6 protein and messenger are highly expressed in GBM and reduced in low malignancy astrocytoma grade II and meningioma. Bcl-6 overexpression is consistent with the degree of apoptosis reduction and with caspase-3 expression. On the contrary, p53 protein and messenger are strongly expressed in GBM as compared to astrocytoma II and meningioma, suggesting a role in inducing cellular damage.

Overall, these results demonstrate that Bcl-6 gene translocation is a common feature of GBM as of PCNSL, and indicate Bcl-6 as a possible gene marker for glioma. They also suggest a putative role for Bcl-6 in the control of tumor cell proliferation and inhibition of apoptosis in glioblastoma.

Materials and methods

Tissue samples

Primary human brain tumors were retrospectively selected from the archive of the Section of Pathology of the University of Torino, Medical School, and the Section of Pathology of the Department of Emergency Surgery and Organ Transplantation of the University of Bari, Medical School. The study was conducted in accordance with local ethics committee guidelines and the Helsinki Declaration. All primary tumors were obtained from patients who had undergone no prior treatment (radiotherapy or chemotherapy) and we showed in Table 1 the clinical, anatomical and molecular features of GBM patients. Tumor type and stage were determined according to the World Health Organization classification[3], using conventional histology. Tumor specimens were obtained from 30 glioblastomas (grade IV), 19 astrocytomas grade III, 17 astrocytomas grade II, 16 PCNLS and 22 meningiomas and 5 healthy tissues, histologically confirmed, from patients who underwent neurosurgical treatments. Tissues were collected at the time of craniotomy, fixed in 10% buffered formalin for 24 h and paraffin-embedded.

4

Table 1.

Clinical, anatomical and molecular features of glioblastoma patients.

Case	Age (years)	Sex	Ki-67 (%)	Tumor location	Bcl6 translocation (%)	Gene expression		
						Bcl6	mIDH1	w/m p53
1	67	M	60	Frontal lobe	40	+	+	+
2	71	M	20	Frontal lobe	−	−	−	+
3	58	F	30	Temporal lobe	−	−	−	±
4	52	M	40	Parieto-occipital lobe	32	+	+	+
5	53	M	20	Thalamo	−	−	−	±
6	38	M	80	Temporal lobe	59	+	+	+
7	64	F	20	Frontal lobe	−	−	−	+
8	67	F	40	Frontal lobe	29	+	+	+
9	57	M	35	Temporo-parietal lobe	−	−	−	+
10	56	M	50	Parieto-occipital lobe	33	+	+	+
11	45	F	25	Left temporal lobe	−	−	−	±
12	80	M	30	Left frontal lobe	20	+	+	+
13	65	M	10	Right parieto-occipital lobe	−	−	−	+
14	81	M	40	Left frontal lobe	23	+	+	+
15	42	M	30	Right temporal lobe	−	−	+	+
16	66	M	40	Right parieto-occipital lobe	−	−	+	±
17	60	M	40	Right temporal lobe	−	−	+	±
18	39	F	30	Left temporal lobe	−	−	−	+
19	54	F	13	Left parieto-occipital lobe	−	−	−	+

Case	Age (years)	Sex	Ki-67 (%)	Tumor location	Bcl6 translocation (%)	Gene expression		
						Bcl6	mIDH1	w/m p53
20	73	M	40	Left parietal lobe	–	–	+	+
21	64	M	25	Left temporo-insular	–	–	+	+
22	60	M	50	Right parietal lobe	37	+	+	+
23	70	F	60	Left fronto-insular	43	+	+	+
24	78	F	13	Left temporal lobe	–	–	–	±
25	43	M	30	Right parieto-occipital lobe	–	–	+	±
26	61	M	20	Left frontal lobe	–	–	–	±
27	46	M	18	Left parietal lobe	–	–	–	+
28	46	M	25	Right temporo-insular	–	–	+	+
29	72	F	60	Occipital lobe	39	+	+	+
30	43	M	50	Parietal lobe	42	+	+	+

Ki-67 tumor proliferative index.

Fish analysis

Interphase FISH was performed on thin sections of formalin-fixed paraffin-embedded (FFPE) tumor samples. All cases were screened for Bcl6 translocation with a two-color break-apart probe (Cytocell, Cambridge, UK). In brief, 4-µm paraffin-embedded sections, mounted on coated slides, were deparaffinized and rehydrated. Slides were next incubated at 96 °C in Tris/EDTA acid buffer solution for 15 min, washed in sterile water and treated in 0.01 N HCl solution at 37 °C for 2 min. Enzymatic digestion was then induced by adding 200 µl 0.4% pepsin (Sigma–Aldrich, St. Louis, MO, USA) solution and incubating at 37 °C for 15 min. Thereafter, tissue samples were washed with sterile water, dehydrated in ethanol, and air dried. The Bcl-6 two-color break-apart probe was used for hybridization according to the manufacturer's protocol. Probe and target were co-denatured at 75 °C for 5 min, followed by overnight hybridization at 37 °C on a StatSpinThermoBrite (Abbott Molecular, Abbott Park, Illinois, USA). Post-hybridization washing was carried out at 72 ± 1 °C in 0.4XSSC for 2 min and in 2XSSC/0.1% Tween at room temperature for 1 min. Then the slides were counterstained and mounted with DAPI-Antifade (Cytocell).

The interphase FISH analysis was performed using an Olympus BX51 fluorescence microscope (Olympus Italia, Rozzano, Italy) with 100X objective lenses and a triple band-pass filter for FITC, Texas Red and DAPI. Images were captured using a high-resolution digital camera (DP70, Olympus Italia) transmitting image data to a PC equipped with appropriate software for images acquisition and analysis (AnalySIS, Olympus Italia).

Hybridization signals were counted in 200 morphologically intact nuclei for each sample.

Signals were considered colocalized when the distance between them was equal to or smaller than the size of one hybridization signal. Only co-localized green and red signals, often resulting in a yellow signal, were considered representative of intact Bcl-6 loci. By contrast, a Bcl-6 translocation breakpoint is easily recognized by the presence of scattered single red and green signals.

Immunofluorescence and fluorescence in situ hybridization analysis (FICTION)

Fluorescence immunophenotyping and interphase cytogenetics (FICTION), a technique combining immunofluorescence and FISH, was carried out on 4-µm-thick paraffin sections of the glioblastoma samples. To identify chromosomal translocations in tumoral cells, FISH assay was performed and then the sections were stained with anti-IDH1 antibody, a cytoplasmic glioblastoma tumoral cells marker which recognizes the isocitrate dehydrogenase 1 (IDH1) R132H point mutation. FISH was performed as described previously. After post-hybridization washing, immunostaining was performed. The tissues were treated with normal goat serum at room temperature for 30 min and incubated overnight with monoclonal mouse anti-human IDH1 R132H (Dianova, Hamburg, Germany) primary antibody at 22 °C, washed in PBS buffer and then incubated at room temperature for 2 h with Alexa Fluor 488 goat anti-mouse (Invitrogen, Carlsbad, CA, USA) antibody, used as secondary reagent. Afterwards, the slides were washed, counterstained with DAPI (Invitrogen), and mounted in Vectashield (Vector Laboratories, Burlingame, CA, USA). Images were captured using an Olympus BX51 microscope fitted with an Olympus DP70 camera, equipped with filter sets for DAPI (nuclei counterstaining), FITC (cytoplasmic immunofluorescence signal and green nuclear FISH signal) and TRITC (red nuclear FISH signal).

Terminal deoxynucleotidyltransferase-mediated dUTP nick end labeling assay-TUNEL test

DNA cleavage was assessed by enzymatic end-labeling of DNA strand breaks using a In Situ Cell Death Detection Kit (Roche, Penzberg, Germany) according to the manufacturer's protocol. Briefly, deparaffinized slides were washed in phosphate-buffered saline (PBS) and permeabilized with 0.1% Triton X-100 and 0.1% sodium citrate for 2 min at 41 °C; after rinsing, slides were incubated with 50 ml of terminal deoxynucleotidyltransferase (TdT)-mediated dUTP nick end labeling (TUNEL) reaction mixture, containing TdT- and FITC-labeled dUTP, in a humidified atmosphere for 1 h at 37 °C in the dark. Afterwards, slides were rinsed and mounted in antifade solution and images were captured as above with a FITC (TUNEL) filter. The percentages of

apoptotic human cells in tumoral sections were evaluated by morphometric analysis carried out on 10 cross reactions from each experimental group, 5 cases per group, using Image Analysis Software (Olympus Italia).

Bcl-6, p53 and caspase 3 Immunohistochemistry

Histological sections of 4 µm thickness, collected on poly- L-lysine-coated slides (Sigma Chemical, St Louis, MO, USA), were deparaffinized and stained in an automated immunostainer (DAKO Autostainer) with a dextran polymer-based system method (EnVision™ Flex+, DAKO) using 3′-3′ diaminobenzidine as chromogen. The sections were rehydrated in a xylene-graded alcohol scale and then rinsed for 10 min in 0.1 M PBS. For p53 and caspase 3 immunodetection, sections were pre-treated with sodium citrate pH 6.1 (Dako Corporation, Milan, Italy) solution for 30 min at 98 °C, for Bcl-6 with EDTA pH8 at the same time and temperature conditions, all in DAKO PT Link for antigen retrieval, and then incubated with monoclonal mouse anti-Bcl-6 (Dako), monoclonal mouse anti-p53 (Dako, Clone DO7), polyclonal rabbit anti-caspase 3 (Novus Biologicals), diluted 1:10, 1:50, 1:100, respectively. Thereafter, the sections were counterstained with Mayer hematoxylin and mounted in synthetic medium. Specific preimmune serum (Dako), replacing the primary antibodies, served as negative control. Morphometric analysis was performed on 10 sections from each experimental group, 5 cases per group, using Image Analysis Software (Olympus Italia).

Real-Time PCR

Total RNA was extracted from FFPE tissue blocks using the RecoverAll™ Total Nucleic Acid isolation kit (Ambion, Life Technologies, Inc., Austin, TX, USA) and then used to synthesize the first-strand c-DNA with the IScriptcDNA Synthesis kit (Bio-Rad Laboratories, Hercules, CA, USA), according to the manufacturer's instructions.

To detect Bcl-6 expression, cDNA was amplified with the iTaq SYBR Green supermix using a ROX kit (Bio-Rad Laboratories, Hercules, CA, USA) while for detection of p53 and caspase 3 expression, cDNA was amplified with the SsoFast Probes Supermix (Bio-Rad Laboratories). PCR amplification was performed using the Chromo4 Real-time PCR Detection System (Bio-Rad Laboratories). Samples were normalized to human RPLPO (large ribosomal protein PO). Table 2 and Table 3 show the sequences of primers (Sigma) used for Bcl-6 amplification and the taqman probes (Applied Biosystems, Life technologies) used for p53 and caspase 3 amplification, respectively.

Table 2.

Primer sequences for real-time PCR.

BCL6/S	5′ CTGCATCAAGCCTCCTC 3′
BCL6/AS	5′ GTTCTCCACCACCTCACG 3′
RPLPO/S	5′ CCTTCCCACTTGCTGAAAAGG 3′
RPLPO/AS	5′ ACAAAGGCAGATGGATCAGCC 3′

Table 3.

TaqMan gene expression assays for real-time PCR.

RPLPO	Hs99999902_m1
CASP3	Hs00234385_m1
TP53	Hs01034253_m1

Protein extraction and Western Blotting

15-µm thick sections were cut for total protein extraction, deparaffinized in xylene, rehydrated in graded ethanol and air-dried. The EXB lysis buffer (QProteome FFPE Tissue kit Qiagen, Hilden, Germany) was added to each samples, and the contents were pre-incubated at 100 C for 20 min before treatment at 80 C for 2 h. After incubation, the tissue lysates were centrifuged at 15,000 g for 20 min at 4°C. The supernatants were collected and stored at −80°C until use for protein assay and Western blot analysis. The protein concentration of the lysates was determined with the Bio-Rad DC Protein Assay (Bio-RadLaboratories, Hercules, CA, USA). For immunoblotting, 30 µg per lane of protein extract were solubilized in Laemmli buffer, boiled at 90°C for 5 min and resolved on a 10% polyacrylamide gel; thereafter, the proteins were electrotransferred to a nitrocellulose membrane (Biorad). Blots were blocked with PBS BB containing 5% non-fat dry milk for 1h and incubated overnight at 4°C with the following primary antibodies: mouse anti-Bcl6 (Santa Cruz) diluted 1:200, mouse anti-p53 (Santa Cruz) diluted 1:100 and mouse anti-RPLPO (Santa Cruz) diluted 1:1000. After the primary antibody treatment, the membranes were washed 4 times for 5min each at RT in PBS/0.1% Tween-20 before the addition of the secondary antibodies. PBS and 0.1% Tween-20-diluted secondary anti-mouse antibodies were IRDye labeled (800CW) (LI-COR Biosciences, Lincoln, NE, USA). For immunoblot analysis, the Li-corOdyssey infrared imaging system was used (LI-COR). The western blot images were analyzed by imaging densitometry using Quantity One Software (Bio-Rad Laboratories) and compared with RPLPO. The data were expressed as optical density/mm^2.

Statistical analysis

Data are reported as means ± SEM. Newman-Keuls multiple comparison post test was used to compare all treatment groups after one-way ANOVA. The Graph Pad Prism 5.0 statistical package (GraphPad Software, San Diego, CA, USA) was used for analyses and the limit for statistical significance was set at $P < 0.05$.

Results

Bcl-6 translocation is correlated with the disease severity

To investigate Bcl-6 translocation in brain tumors with different degrees of malignancy, (Table 1 and Table 4) interphase FISH analysis and FICTION technique, on thin sections of the FFPE tumor samples, were performed. The FICTION technique detected red and green separate fluorescent spots in the nuclei of glioblastoma IDH1 positive cells (white asterisk), indicating Bcl-6 translocation, (Fig. 1A and B), while close red and green fluorescent signals were present in IDHL-1-negative cells (Fig. 1C). Therefore, in glioblastomas positive IDH1 tumor cells are carriers of the Bcl-6 translocation.

Table 4.

Molecular features of different type of glioma tumors.

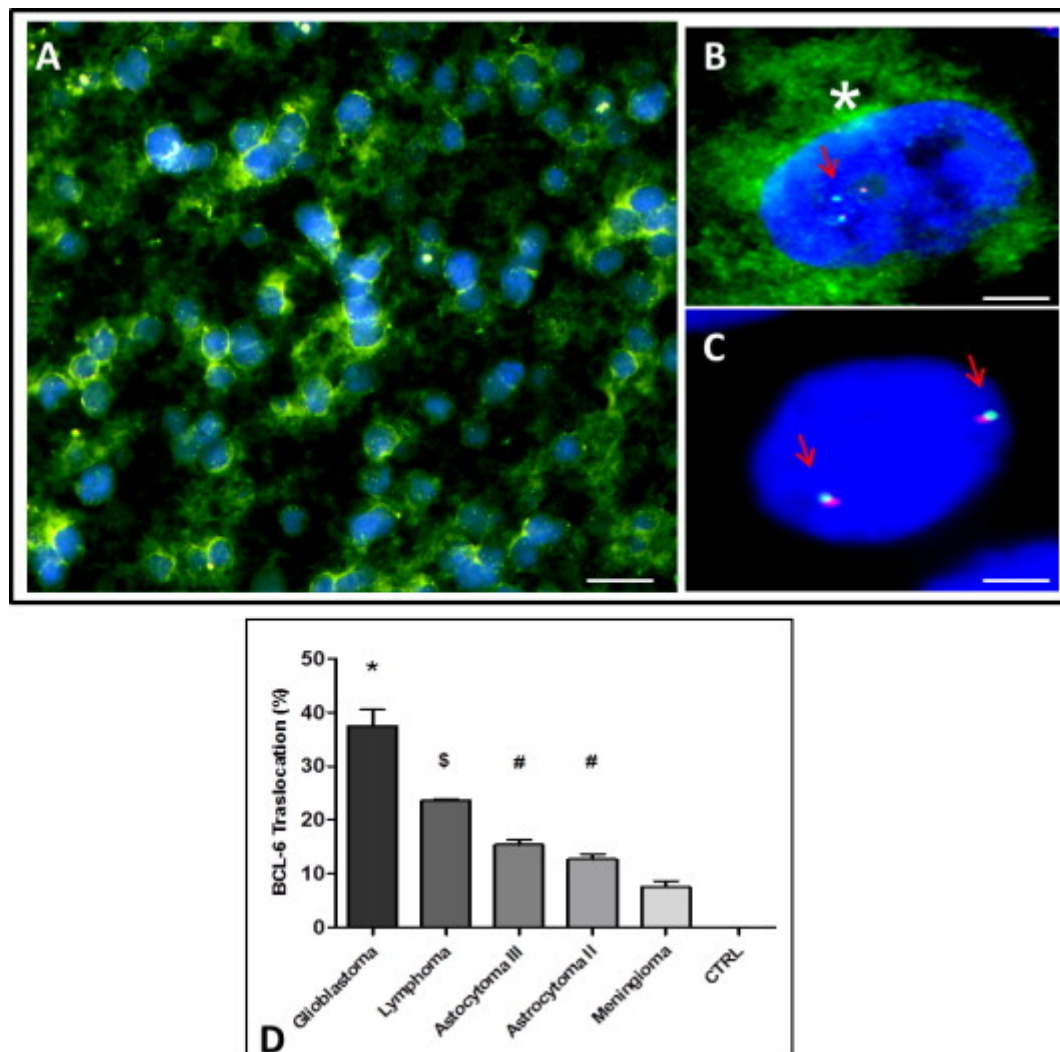| Glioma histology	Number of Patients	mIDH1 expression		Bcl6 translocation		Bcl6 expression	w/mp53 expression
		Yes	%	Yes	%	Yes	Yes
Glioblastoma grade IV	30	18	60	11	36.6	11	30
Astrocitoma grade III	19	2	11.7	3	15.8	3	19
Astrocitoma grade II	17	3	15.7	2	11.8	2	17
Meningioma	22	0	0	2	9	1	22

10

Fig. 1.

Bcl-6 translocation in glioblastoma patients by FICTION (A–C) and fluorescence in situ hybridization (FISH) (D) analysis on paraffin sections. (A and B) IDH1 green labeled tumoral cells (B, asterisk) show a red and green separate fluorescent spots in the nucleus (B, arrow) indicating a Bcl-6 translocation. (C) IDH1 negative cell shows a normal nucleus with close red and green fluorescent signals, indicating no Bcl-6 translocation. (D) Interphase FISH analysis shows a significant increase of Bcl-6 mutations in glioblastoma patients ($36.6\% \pm$ SE 3.059), a significant reduction in lymphomas ($23.63\% \pm$ SE 0.25) and astrocytomas grade III ($15.78 \pm$ SE 0.92) and grade II ($11.76 \pm$ SE 1.02) and a return to basal conditions in meningiomas ($9\% \pm$ SE 1.17). $^{*}p < 0.05$ vs other groups, $^{\$}p < 0.05$ vs meningiomas and control groups, $^{\#}p < 0.05$ vs control. Scale bar: A, 25 µm; B and C, 10 µm. (For interpretation of the references to color in this figure legend, the reader is referred to the web version of this article.)

11

Interphase FISH analysis showed a significant parallel increase of the Bcl-6 mutation with the degree of disease malignancy as compared to meningioma and healthy controls.

In glioblastoma grade IV, rearrangement of Bcl-6 showed a frequency of 36.6% ± SE 3.05%, versus a significant decrease, to 15.78% ± SE 0.92 and 11.76% ± SE 1.02%, in astrocytomas grade III and grade II, respectively. In meningioma sections the Bcl-6 mutation was present only in 9% ± ES 1.17% and decreased to 0% in healthy controls (Fig. 1D). In the PCNSL sections, used as positive controls, the translocation frequency was 23.63% ± ES 0.25%. Table 1 and Table 4 showed number of patients positive for Bcl-6 translocation and mIDH1 expression in different type of glioma tumors.

Bcl-6 gene expression is correlated with the severity of the disease

To assess the Bcl-6 expression pattern, immunohistochemistry, western blotting analysis and Real Time-PCR assay were performed. As shown in Fig. 2(A–D), a strong immunocytochemical nuclear expression of Bcl-6 was seen in glioblastoma (A) specimens, while a reduction of Bcl-6 expression in astrocytoma grade III (B), PCNSL (C) and meningioma specimens (D) was detected. Morphometric analysis showed a significant difference in Bcl-6 expression between glioblastomas and PCNSL compared with astrocytoma grades II and III, meningiomas and controls patients (Fig. 2E). Western blotting analysis confirmed an overexpression of Bcl-6 protein in the tumor samples as compared to controls and significantly higher protein content levels in glioblastoma as compared with the other tumors (Fig. 3A and B).
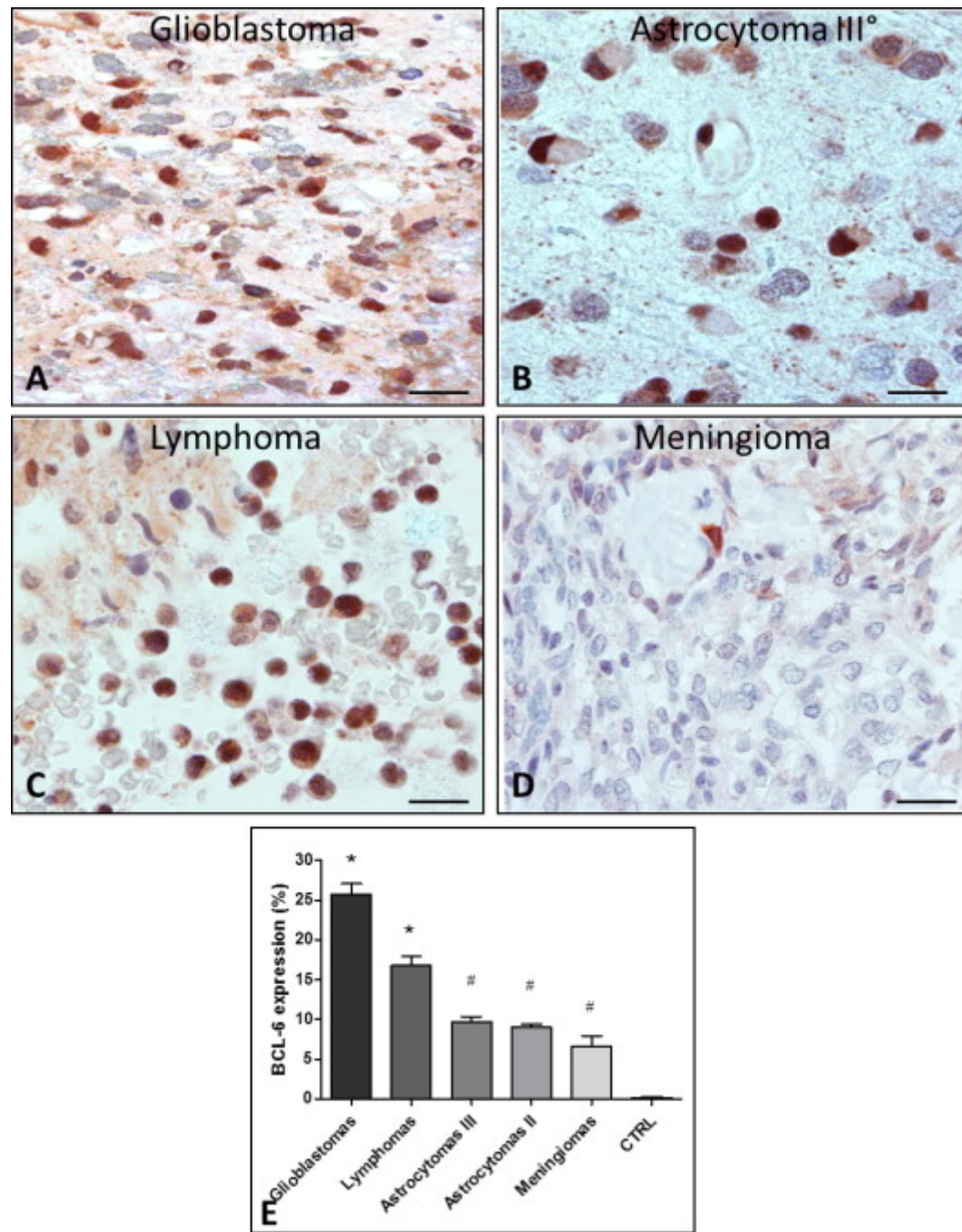
Fig. 2.

Bcl-6 immunohistochemistry (A–D) and morphometric analysis (E). Glioblastoma sections show a strong Bcl-6 nuclear expression (A), which is reduced in grade III astrocytoma (B), lymphoma (C) and meningioma (D) sections. Morphometric analysis (E) reveals a significative increase of Bcl6 protein in glioblastomas (25.75% ± SE 0.75) and lymphoma cases(16.77% ± SE 0.67), compared to astrocytomas grade III (9.17% ± SE 0.36), astrocytomas grade II ((9.02% ± SE 0.24) and meningiomas (6.64% ± SE 0.75) cases. No Bcl6 protein is present in control (*p < 0.001 *vs* all groups, #p < 0.001 vs control). Scale bar A–D, 25 μm.
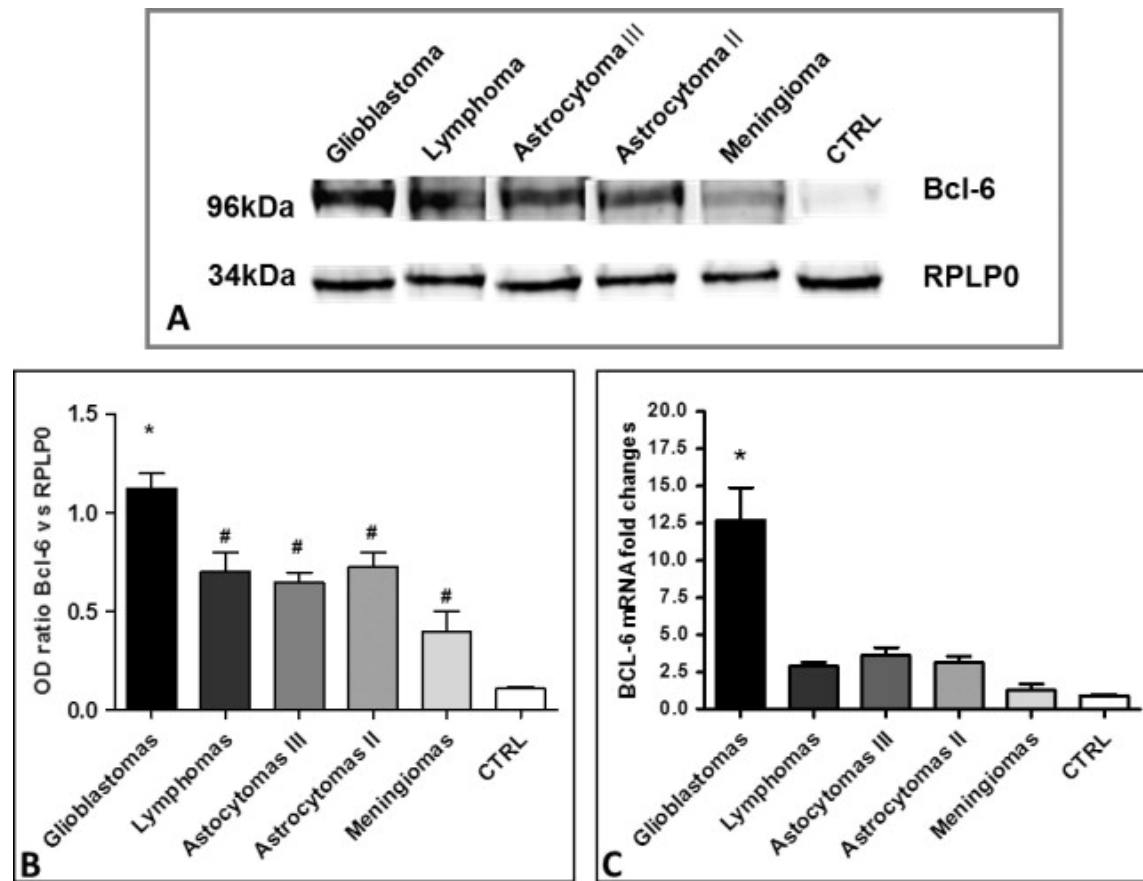
13

Fig. 3.

Bcl-6 protein (A and B) and messenger (C) expression analysis Western blotting analysis (A and B) shows a high Bcl-6 expression in glioblastoma (1.12 ± SE 0.07) patients, and a significant reduction in lymphoma (0.70 ± SE 0.10), astrocytomas grade III (0.65 ± SE 0.05), astrocitomas grade II (0.72 ± SE 0.07), meningiomas (0.40 ± SE 0.10), and control brain (0.11 ± SE 0.01) ($^{*}p < 0.05$ vs other groups, $^{\#}p < 0.05$ vs control). The RT–PCR analysis (C) shows a significant Bcl-6 overexpression in glioblastomas (12.71 ± SE 2.17) as compared to lymphomas (2.89 ± SE 0.25), astrocytomas grade III (3.64 ± SE 0.51) and II (3.16 ± SE 0.42), meningiomas (1.31 ± SE 0.38) and to healthy brain (0.93 ± SE 0.07) ($^{*}p < 0.05$ vs other groups).

After Real Time-PCR (Fig. 3C), Bcl-6 mRNA was highly expressed in glioblastoma (12.71 ± SE 2.17) and significantly ($P < 0.05$) decreased in PCNSL (2.89 ± SE 0.25), astrocytoma grade III (3.65 ± SE 0.52) and grade II (3.16 ± SE 0.04) and in meningioma (1.32 ± SE 0.38) specimens. Bcl-6 mRNA was not detectable in the healthy brain tissues.

Bcl-6 protein promotes tumor cells proliferation through the inhibition of apoptosis and caspase-3 expression

Bcl-6 is a transcriptional factor that induces cell proliferation and reduces apoptosis. We evaluated the degree of apoptosis in gliomas, PCNSL and meningiomas specimens, by means of the TUNEL assay and caspase-3 expression.

As shown in Fig. 4(A–D), the TUNEL assay, which measures DNA strand breaks in individual cells, revealed no apoptosis in glioblastoma (A) and only few fluorescent apoptotic cells present in PCNSL (B) and in astrocytoma grade II (C) sections, whereas brighter green fluorescent cells were recognizable in meningiomas (D). Morphometric analysis demonstrated a lower percentage of apoptotic cells in glioblastomas (0.32% ± SE 0.09), PCNSL (0.7% ± SE 0.08) and astrocytomas grade III (0.99% ± SE 0.46) as compared to astrocytomas grade II (1.69% ± SE 0.52) and meningiomas (2.53% ± SE 0.18) (Fig. 4E). The difference in apoptotic cells between aggressive and less aggressive tumors was significant ($P < 0.05$) and correlated with differences in Bcl-6 expression.
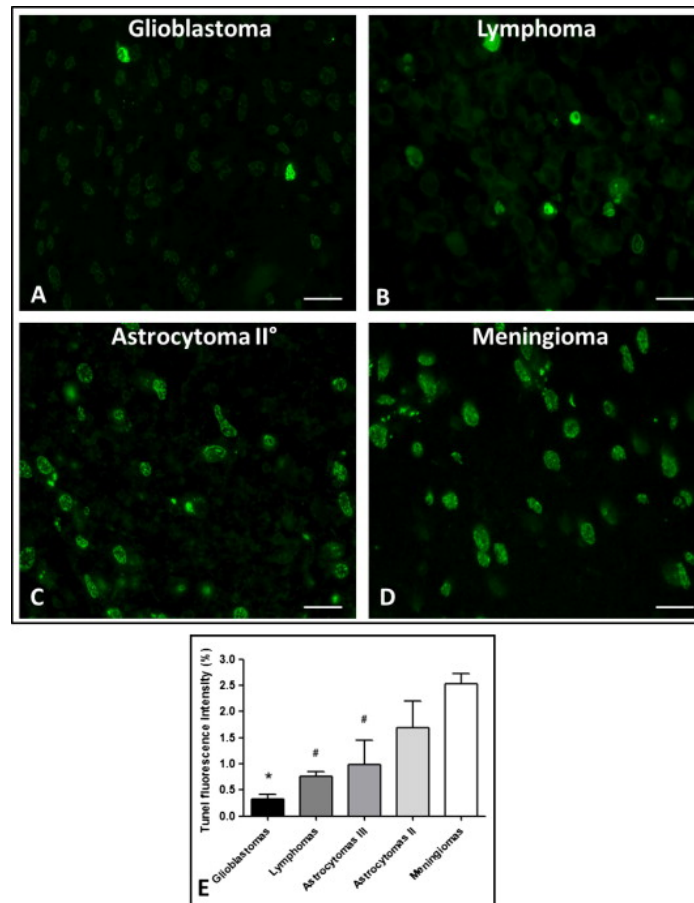
Fig. 4.

Apoptosis analysis. TUNEL assay shows no apoptosis in glioblastoma (A) and a progressive increase of fluorescent apoptotic cells in PCNSL (B), astrocytoma grade II (C) and in meningioma (D) sections. (E) Morphometric analysis reveals a lower percentage of apoptotic cells in glioblastomas ($0.32\% \pm$ SE 0.09), lymphomas ($0.7\% \pm$ SE 0.08) and grade III astrocytomas ($0.99\% \pm$ SE 0.46) as compared to astrocytomas grade II ($1.69\% \pm$ SE 0.52) and meningiomas. ($2.53\% \pm$ SE 0.18) ($^{*}p < 0.05$ vs astrocitomas and meningiomas groups, $^{\#}p < 0.05$ vs meningiomas group). Scale bar, 16.6 µm.

After caspase-3 immunohistochemical staining, in accordance with the TUNEL test results, a few labeled tumor cells were detected in glioblastoma, astrocytoma grade III and PCNSL sections (Fig. 5A–C) as compared with astrocytoma II and low meningioma (Fig. 5D and E). No caspase expression was detectable in healthy brain specimens (Fig. 5F). Morphometric analysis confirmed a significant difference in caspase-3 expression between meningioma and astrocytoma grade II as compared with glioblastoma, PCNSL and astrocytoma grade III (Fig. 5G).
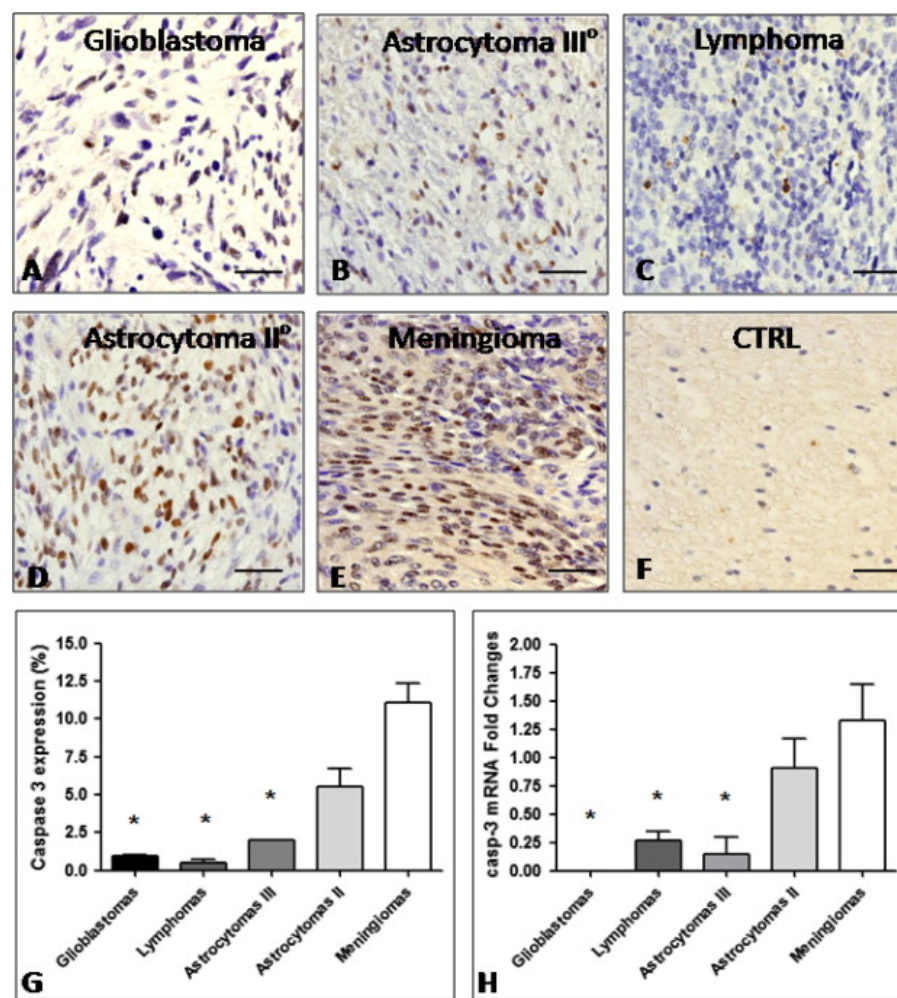
Fig. 5.

Caspase-3 immunohistochemistry (A–G) and gene expression analysis (H). Glioblastoma (A), astrocytoma III (B) and PCNSL (C) sections show a lower expression of caspase-3, which is significantly increased in astrocytoma grade II (D) and meningioma (E) sections No caspase-3 expression is revealed in healthy brain controls (F). ($^{*}p < 0.05$ vs astrocytoma and meningioma groups). Morphometric analysis (G) reveals a lower caspase-3 expression in glioblastomas (0.98% ± SE 0.03), lymphomas (0.49% ± SE 0.22) and astrocytomas grade III (2% ± SE 0.02) as compared to astrocytomas grade II (5.49% ± SE 1.26) and meningiomas (11.10% ± SE 1.23). RT–PCR analysis (H) shows a strong expression of caspase-3 in meningiomas (1.32 ± SE 0.32) and astrocytomas grade II (0.91 ± SE 0.25), and a significant decrease in astrocytomas grade III (0.15 ± SE 0.15) and PCNSL (0.26 ± ES 0.08). No caspase-3 mRNA is present in glioblastoma ($^{*}p < 0.05$ vs astrocytomas II and meningiomas groups). Scale bar, A–F 25 µm.

After Real Time-PCR (Fig. 5H), caspase-3 mRNA was most strongly expressed in meningiomas (1.32 ± SE 0.32) and astrocytomas grade II (0.91 ± SE 0.26), and significantly ($P < 0.05$) decreased in astrocytomas grade III (0.15 ± SE 0.15) and in PCNSL (0.26 ± SE 0.08). No caspase-3 mRNA was detected in glioblastoma sections.

Bcl-6 and p53 protein expression are correlated

We also studied p53 expression in the brain tumor specimens, since Bcl-6 is a gene promoter involved in p53 protein regulation. After immunohistochemistry and Real Time-PCR we found a high p53 protein expression and mRNA content in glioblastoma and astrocytoma grade III (Fig. 6A, B, E and F) and a significantly decreased expression in astrocytoma grade II (Fig. 6C, E and F) and meningioma (Fig. 6D–F) specimens. p53 protein and mRNA were not detectable in the in healthy brain tissues (Fig. 6E and F). Western blotting analysis confirmed a p53 protein overexpression in the tumor samples as compared to controls, and significantly higher protein content levels in glioblastoma as compared with the other tumors (Fig. 7A and B). Table 1 and Table 4 showed number of patients positive for wt/m p53 expression in different type of glioma tumors.
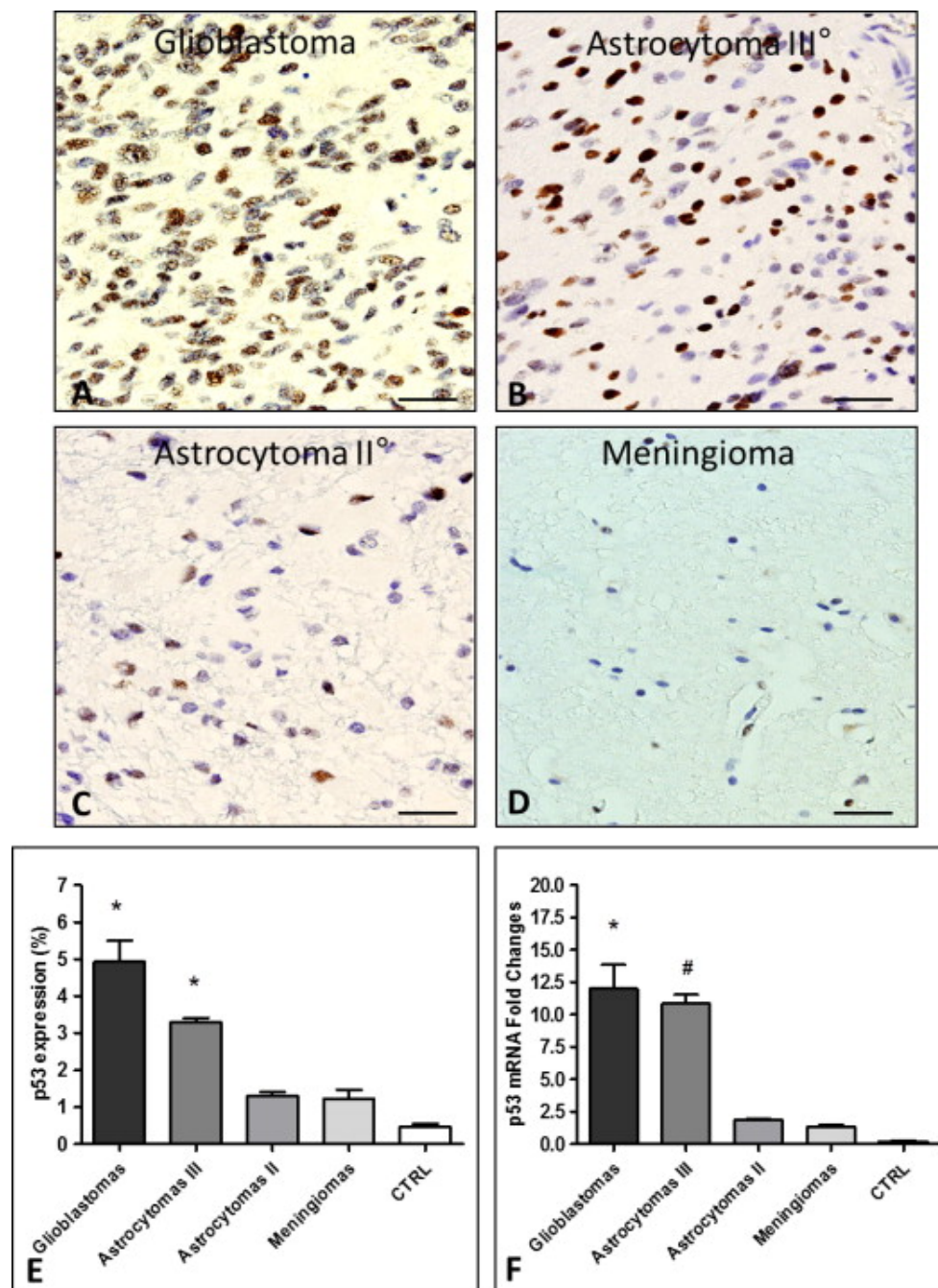
17

Fig. 6.

p53 immunohistochemistry (A–E), and gene expression analysis (F). Glioblastoma (A) and astrocytoma grade III (B) sections show numerous p53-labeled tumor cells, which are significantly decreased in grade II astrocytoma (C) and meningioma (D) sections. Morphometric analysis (E) confirms significative reduction of p53 protein from glioblastomas (4.93% ± SE 0.56) and astrocytomas grade III (3.30% ± SE 0.10) cases to astrocytomas grade II (1.30 ± SE 0.10) meningiomas (1.26% ± SE 0.24) and control brain (0.46% ± SE 0.08). ($^*p$ < 0.05 glioblastoma and astrocytoma grade III vs all groups). RT–PCR analysis (F) shows that p53 is significantly overexpressed in

18

glioblastomas ($12.0 \pm$ SE 1.84) and astrocytomas grade III ($10.85 \pm$ SE 0.7) as compared to astrocytomas grade II ($1.83 \pm$ SE 0.07), meningiomas ($1.37 \pm$ SE 0.16) and healthy brain ($0.15 \pm$ SE 0.07) ($^*p < 0.05$ glioblastoma vs astrocytoma grades II, meningioma, and control brain; $^\#p < 0.05$ astrocytoma grade III vs astrocytoma grade II, meningiomas, and control brain). Scale bar, A–D 25 μm.
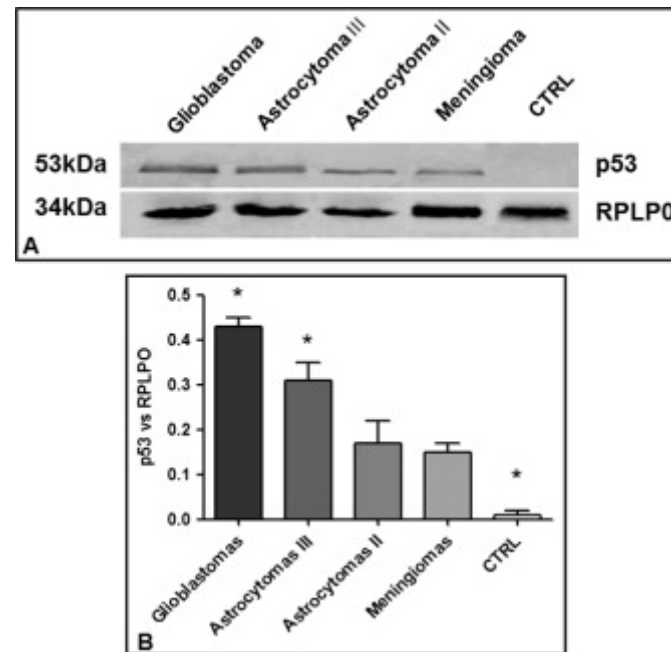

Fig. 7.

p53 protein expression analysis (A and B). Western blotting analysis shows a high p53 expression in glioblastoma $0.43 \pm$ SE 0.01) patients, and a significant reduction in astrocytomas grade III ($0.31 \pm$ SE 0.02), astrocytomas grade II ($0.17 \pm$ SE 0.03) meningiomas ($0.15 \pm$ SE 0.01), and control brain($0.01 \pm$ SE 0.0) ($^*p < 0.05$ vs other groups).

Discussion

In this study, we have demonstrated the presence of Bcl6 translocation in glioma brain tumors and confirmed the incidence in PCNSL. In addition, we have shown a correlation between the frequency of Bcl6 translocation and tumor aggressiveness, suggesting a potential role for this gene in tumorigenesis. The Bcl6 gene is fully expressed only in germinal centers, where it induces proliferation and differentiation of B and CD4^{+} T

19

cells[22] and [23] and contributes to the regulation of immune responses[24]. The two common genomic alterations, translocations and somatic mutations, affecting this gene, may lead to a deregulation of B-cell maturation and contribute to lymphomagenesis[25] and[26.] This gene is normally silent or expressed at low levels in a wide variety of tissues but its translocation leads to substitution of the Bcl6 promoter by heterologous sequences derived from the different translocation partners, resulting in constitutive expression of the Bcl6 gene[10] and[27]. We found that Bcl6 translocations are recurrent in the nuclei of glioblastoma IDH1 cells confirming that this mutation is related to tumorigenesis. Somatic mutations of IDH1 are frequently observed in grade II and III gliomas and secondary glioblastomas[28] and[29]. The IDH1 gene encodes isocitrate dehydrogenase 1 which catalyzes the oxidative carboxylation of isocitrate to α-ketoglutarate, resulting in the production of NADPH in the Krebs cycle[30]. IDH1 mutations, resulting in amino acid substitutions at a single arginine residue, inhibit wild-type IDH1 activity[31]. The cytosolic expression of mutant IDH1 reduces the formation of α-ketoglutarate and increases the levels of the hypoxia-inducible factor (HIF-1α) subunit, leading to vascular endothelial growth factor (VEGF) expression, which induces tumor angiogenesis[32] and[33].

Furthermore, we have demonstrated, for the first time in brain tumors, a significant increase of Bcl6 expression at both transcriptional and translational levels, and its correlation with the gene rearrangement and the degree of tumor malignancy. RT–PCR, Western Blotting and immunohistochemistry analysis shows that Bcl6 is significantly overexpressed in grade IV glioma as compared to PCNSL, to grade III and II astrocytoma, to meningioma and to healthy brain. Numerous targets of Bcl6 suppressive effects have been identified, including genes implicated in B cell activation and differentiation, inflammation, cell cycle, DNA repair, chromatin formation, transcriptional regulation, and protein stability, in both normal and malignant B cells3[4] and [35]. Furthermore, Bcl6 can repress several oncogenes and interact with various co-repressors in order to repress genes involved in a variety of different biologic pathways[35]. Certainly, deregulation of Bcl6 results in perturbation of the proteins that control apoptosis; some works have shown that a high expression of Bcl6 induces apoptosis[36] and[37], while others found that Bcl-6 protects the cells from apoptosis[34], [38], [39] and [40]. The precise role of Bcl-6 in enhancing or inhibiting apoptosis is still unclear.

In this study we have shown that Bcl-6 plays a role in the repression of apoptosis in human cancer cells, and that at least one mechanism through which this occurs is by inactivating caspase 3, a key protein in the cascade of events leading to apoptosis. We have demonstrated that a reduced apoptosis is correlated with rearrangement of the gene and with the degree of tumor malignancy. In fact, in the cancer cells of glioblastoma, apoptosis is almost absent, while it rises in the tumor cells of PCNSL, grade III and II astrocytomas and is significantly increased in meningiomas. In support of these findings, Real Time and immunohistochemical studies in human benign meningiomas and in gliomas show that the expression of Bcl-6 and of caspase 3 is inversely correlated in these tumors, Bcl-6 expression being high but caspase-3 low or not detectable. The Bcl-6 transcript and the related protein are more strongly expressed in glioblastoma than in other glioma tumors and PCNSL, although Bcl-6 expression is indicative of the latter disease.

20

Several studies have reported that the p53 tumor suppressor gene is directly targeted by Bcl-6[41]. Bcl-6 suppresses p53 gene expression and modulates DNA damage-induced apoptotic responses in germinal-center B cells facilitating expansion[41]. p53 is activated in response to a variety of cellular and genotoxic stress conditions, leading to the induction of growth arrest, apoptosis, DNA repair, senescence, and differentiation[42]. However, several studies obtained contradictory results regarding the relationship between p53 and Bcl-6 expression. Although Bcl-6 can directly repress p53 in the germinal center, we have found that the p53 gene is expressed in gliomas as a translated transcript, and that it is also more strongly expressed in glioblastomas in correlation with Bcl-6 expression. This observation suggests that repression of Bcl-6 target genes, such as p53, is partly dependent on the cellular context [43]. The fact that both mRNA and protein are increased in the presence of Bcl6 is consistent with previous reports showing that several types of cellular stress can cause a similar effect [44]and [45]. Shvarts et al. [46] reported that Bcl6 might be able to bypass induced senescence in primary mouse embryonic fibroblasts and in a mixed population of human B-cells, and that Bcl6-mediated induction of cyclin D1 could explain this effect. We hypothesize that, unlike in germinal centers, in glioblastoma tissues the cells are unable to evade the p53 response to Bcl6 including growth arrest and senescence. Ranuncolo et al. [47] reported that when B-cells transit through the germinal center they acquire the ability to evade p53 checkpoint activity, which is not entirely dependent on the repressor activity of Bcl6, but can be mediated by some still unknown factor. Similarly to Bcl-6 expression, higher p53 levels were recorded in immunoproliferative small intestinal disease cases with a poor outcome, whereas a lower level was found in other cases in remission at follow-up [48]. Moreover, a mutant form of p53 is overexpressed by many malignant tumors including lymphomas and glioblastomas [2] and [49].

Taken together, these data indicate that even if p53 is overexpressed, it is likely not functional, being mutated or because the apoptosis inhibitor action of BCL6 is predominant in tumors such as glioblastoma. Furthermore, Margalit et al. [50] identified Bcl-6 as a new target gene of p53 and showed that the Bcl-6 gene contains a p53 response element (RE) residing within the chromosomal translocations, point mutations, and deletions region in B-cell non Hodgkin lymphoma. But in contrast to these authors' hypotheses, we postulate that this novel p53-bcl6 auto-regulatory loop could allow p53 suppression of Bcl-6, then inducing apoptosis and repairing cell damage in physiological conditions. We also assume that p53 binding to the RE is abrogated in glioblastoma cases due to the Bcl-6 translocation located in the RE, resulting in a deregulation of Bcl-6 expression. Thus, the translocation of Bcl6 not only allows the gene to be transcribed from a new coding sequence but also to evade the suppression induced by p53 in human gliomas is present as a protein and as a messenger but does not exert its function, while Bcl6 inhibits apoptosis and so allows proliferation of tumor cells. In this scenario, in germinal centers p53 is activated upon induction of cell proliferation induced by Bcl-6 and in response to the breaks formed in the genomic DNA due to Ig gene somatic hypermutation and class switch recombination [51] and[52]. Thereby, p53 limits the oncogenic potential of these breaks and down-regulates Bcl-6, causing a return to baseline levels and defining a tightly controlled time window for the completion of B-cell maturation. In this time window, during successive differentiation cycles Bcl-6 may temporarily inhibit p53 from promoting apoptosis and preventing cell proliferation. Thus,

while in germinal centers p53 and Bcl-6 are antagonists with different expression levels depending on the cell cycle phase, in glioma tumors the expression of Bcl-6 and p53 is correlated, and increased in relation to Bcl-6 translocation and the tumor aggressiveness.

Although previous studies have reported that translocations may indicate a favorable prognosis[20,21]and [53], an unfavorable prognosis[17]and [54], or no effect [14]and [21], in our study, Bcl-6 translocation combined with a high expression of Bcl-6 and p53 genes appears to be a poor prognostic indicator and a potential new gene marker for gliomas.

Finally, we suggest that, in these conditions of elevated p53 expression, gene therapy experiments could be conducted to induce apoptosis and reduce the tumor aggressiveness, through a re-establishment of the regulatory loop of Bcl-6 and its basal conditions.

Future research directions will aim to identify potential partner genes for Bcl6 translocation as well as functional studies in glioma cells carrying or not Bcl-6 translocation to validate the presence of the p53-Bcl-6 auto-regulatory loop involved in gliomagenesis processes.

Conflict of Interest

There is no conflict of interest.

Acknowledgement

References

1. F.B. Furnari, T. Fenton, R.M. Bachoo, A. Mukasa, J.M. Stommel, A. Stegh, W.C. Hahn, K.L. Ligon, D.N. Louis, C. Brennan, L. Chin, R.A. DePinho, W.K. Cavenee Malignant astrocytic glioma: genetics, biology, and paths to treatment Genes Dev., 21 (2007), pp. 2683–2710
2. E.A. Maher, F.B. Furnari, R.M. Bachoo, D.H. Rowitch, D.N. Louis, W.K. Cavenee, R.A. DePinho Malignant glioma: genetics and biology of a grave matter Genes Dev., 15 (2001), pp. 1311–1333
3. D.N. Louis, H. Ohgaki, O.D. Wiestler, W.K. Cavenee, P.C. Burger, A. Jouvet, B.W. Scheithauer, P. Kleihues The 2007 WHO classification of tumors of the Central Nervous System Acta Neuropathol., 114 (2007), pp. 97–109
4. H. Ohgaki, P. Dessen, B. Jourde, S. Horstmann, T. Nishikawa, P.L. Di Patre, C. Burkhard, D. Schuler, N.M. Probst-Hensch, P.C. Maiorka, N. Baeza, P. Pisani, Y. Yonekawa, M.G. Yasargil, U.M. Lutolf, P. Kleihues Genetic pathways to glioblastoma: a population-based study Cancer Res., 64 (2004), pp. 6892–6899

22

5. T. Homma, T. Fukushima, S. Vaccarella, Y. Yonekawa, P.L. Di Patre, S. Franceschi, H. Ohgaki Correlation among pathology, genotype, and patient outcomes in glioblastoma J. Neuropathol. Exp. Neurol., 65 (2006), pp. 846–854

6. K. Bansal, M.L. Liang, J.T. Rutka Molecular biology of human gliomas Technol. Cancer Res. Treat., 5 (2006), pp. 185–194

7. D.W. Parsons, S. Jones, X. Zhang, J.C. Lin, R.J. Leary, P. Angenendt, P. Mankoo, H. Carter, I.M. Siu, G.L. Gallia, A. Olivi, R. McLendon, B.A. Rasheed, S. Keir, T. Nikolskaya, Y. Nikolsky, D.A. Busam, H. Tekleab, L.A. Diaz Jr., J. Hartigan, D.R. Smith, R.L. Strausberg, S.K. Marie, S.M. Shinjo, H. Yan, G.J. Riggins, D.D. Bigner, R. Karchin, N. Papadopoulos, G. Parmigiani, B. Vogelstein, V.E. Velculescu, K.W. Kinzler An integrated genomic analysis of human glioblastoma multiforme Science, 321 (2008), pp. 1807–1812

8. S. Nobusawa, T. Watanabe, P. Kleihues, H. Ohgaki IDH1 mutations as molecular signature and predictive factor of secondary glioblastomas Clin. Cancer Res.: Official J. Am. Assoc. Cancer Res., 15 (2009), pp. 6002–6007

9. Y. Liu, W. Jiang, J. Liu, S. Zhao, J. Xiong, Y. Mao, Y. Wang IDH1 mutations inhibit multiple alpha-ketoglutarate-dependent dioxygenase activities in astroglioma J. Neurooncol., 109 (2012), pp. 253–260

10. B.H. Ye, F. Lista, F. Lo Coco, D.M. Knowles, K. Offit, R.S. Chaganti, R. Dalla-Favera Alterations of a zinc finger-encoding gene, BCL-6, in diffuse large-cell lymphoma Science, 262 (1993), pp. 747–750

11. I.S. Lossos, T. Akasaka, J.A. Martinez-Climent, R. Siebert, R. Levy The BCL6 gene in B-cell lymphomas with 3q27 translocations is expressed mainly from the rearranged allele irrespective of the partner gene Leukemia, 17 (2003), pp. 1390–1397

12. D. Allman, A. Jain, A. Dent, R.R. Maile, T. Selvaggi, M.R. Kehry, L.M. Staudt BCL-6 expression during B-cell activation Blood, 87 (1996), pp. 5257–5268

13. W. Chen, S. Iida, D.C. Louie, R. Dalla-Favera, R.S. Chaganti Heterologous promoters fused to BCL6 by chromosomal translocations affecting band 3q27 cause its deregulated expression during B-cell differentiation Blood, 91 (1998), pp. 603–607

14. Bastard, C. Deweindt, J.P. Kerckaert, B. Lenormand, A. Rossi, F. Pezzella, C. Fruchart, C. Duval, M. Monconduit, H. Tilly LAZ3 rearrangements in non-Hodgkin's lymphoma: correlation with histology, immunophenotype, karyotype, and clinical outcome in 217 patients Blood, 83 (1994), pp. 2423–2427

15. B.H. Ye, S. Chaganti, C.C. Chang, H. Niu, P. Corradini, R.S. Chaganti, R. Dalla-Favera Chromosomal translocations cause deregulated BCL6 expression by promoter substitution in B cell lymphoma EMBO J., 14 (1995), pp. 6209–6217

16. F.M. Cady, B.P. O'Neill, M.E. Law, P.A. Decker, D.M. Kurtz, C. Giannini, A.B. Porter, P.J. Kurtin, P.B. Johnston, A. Dogan, E.D. Remstein Del(6)(q22) and BCL6 rearrangements in primary CNS lymphoma are indicators of an aggressive clinical course J. Clin. Oncol.: Official J. Am. Soc. Clin. Oncol., 26 (2008), pp. 4814–4819

17. S.L. Barrans, S.J. O'Connor, P.A. Evans, F.E. Davies, R.G. Owen, A.P. Haynes, G.J. Morgan, A.S. Jack Rearrangement of the BCL6 locus at 3q27 is an independent poor prognostic factor in nodal diffuse large B-cell lymphoma Br. J. Haematol., 117 (2002), pp. 322–332

18. F. Lo Coco, B.H. Ye, F. Lista, P. Corradini, K. Offit, D.M. Knowles, R.S. Chaganti, R. Dalla-Favera Rearrangements of the BCL6 gene in diffuse large cell non-Hodgkin's lymphoma Blood, 83 (1994), pp. 1757–1759

19. T. Otsuki, T. Yano, H.M. Clark, C. Bastard, J.P. Kerckaert, E.S. Jaffe, M. Raffeld Analysis of LAZ3 (BCL-6) status in B-cell non-Hodgkin's lymphomas: results of rearrangement and gene expression studies and a mutational analysis of coding region sequences Blood, 85 (1995), pp. 2877–2884

20. M. Jerkeman, P. Aman, E. Cavallin-Stahl, E. Torlakovic, M. Akerman, F. Mitelman, T. Fioretos Prognostic implications of BCL6 rearrangement in uniformly treated patients with diffuse large B-cell lymphoma–a Nordic Lymphoma Group study Int. J. Oncol., 20 (2002), pp. 161–165

21. M.H. Kramer, J. Hermans, E. Wijburg, K. Philippo, E. Geelen, J.H. van Krieken, D. de Jong, E. Maartense, E. Schuuring, P.M. Kluin Clinical relevance of BCL2, BCL6, and MYC rearrangements in diffuse large B-cell lymphoma Blood, 92 (1998), pp. 3152–3162

22. K. Basso, R. Dalla-Favera Roles of BCL6 in normal and transformed germinal center B cells Immunol. Rev., 247 (2012), pp. 172–183

23. G. Cattoretti, C.C. Chang, K. Cechova, J. Zhang, B.H. Ye, B. Falini, D.C. Louie, K. Offit, R.S. Chaganti, R. Dalla-Favera BCL-6 protein is expressed in germinal-center B cells Blood, 86 (1995), pp. 45–53

24. B.H. Ye, G. Cattoretti, Q. Shen, J. Zhang, N. Hawe, R. de Waard, C. Leung, M. Nouri-Shirazi, A. Orazi, R.S. Chaganti, P. Rothman, A.M. Stall, P.P. Pandolfi, R. Dalla-Favera The BCL-6 proto-oncogene controls germinal-centre formation and Th2-type inflammation Nat. Genet., 16 (1997), pp. 161–170

25. A.L. Dent, A.L. Shaffer, X. Yu, D. Allman, L.M. Staudt Control of inflammation, cytokine expression, and germinal center formation by BCL-6 Science, 276 (1997), pp. 589–592

26. G. Cattoretti, L. Pasqualucci, G. Ballon, W. Tam, S.V. Nandula, Q. Shen, T. Mo, V.V. Murty, R. Dalla-Favera Deregulated BCL6 expression recapitulates the pathogenesis of human diffuse large B cell lymphomas in mice Cancer Cell, 7 (2005), pp. 445–455

27. T. Akasaka, I. Miura, N. Takahashi, H. Akasaka, N. Yonetani, H. Ohno, S. Fukuhara, M. Okuma A recurring translocation, t(3; 6)(q27; p21), in non-Hodgkin's lymphoma results in replacement of the 5′ regulatory region of BCL6 with a novel H4 histone gene Cancer Res., 57 (1997), pp. 7–12

28. H. Yan, D.W. Parsons, G. Jin, R. McLendon, B.A. Rasheed, W. Yuan, I. Kos, I. Batinic-Haberle, S. Jones, G.J. Riggins, H. Friedman, A. Friedman, D. Reardon, J. Herndon, K.W. Kinzler, V.E. Velculescu, B. Vogelstein, D.D. Bigner IDH1 and IDH2 mutations in gliomas New England J. Med., 360 (2009), pp. 765–773

29. J. Balss, J. Meyer, W. Mueller, A. Korshunov, C. Hartmann, A. von Deimling Analysis of the IDH1 codon 132 mutation in brain tumors Acta Neuropathol., 116 (2008), pp. 597–602

30. B.V. Geisbrecht, S.J. Gould The human PICD gene encodes a cytoplasmic and peroxisomal NADP(+)-dependent isocitrate dehydrogenase J. Biol. Chem., 274 (1999), pp. 30527–30533

31. D.T. Hartong, M. Dange, T.L. McGee, E.L. Berson, T.P. Dryja, R.F. Colman Insights from retinitis pigmentosa into the roles of isocitrate dehydrogenases in the Krebs cycle Nat. Genet., 40 (2008), pp. 1230–1234

32. Fischer, J.P. Gagner, M. Law, E.W. Newcomb, D. Zagzag Angiogenesis in gliomas: biology and molecular pathophysiology Brain Pathol., 15 (2005), pp. 297–310

33. T. Acker, K.H. Plate Hypoxia and hypoxia inducible factors (HIF) as important regulators of tumor physiology Cancer Treat. Res., 117 (2004), pp. 219–248

34. A.L. Shaffer, X. Yu, Y. He, J. Boldrick, E.P. Chan, L.M. Staudt BCL-6 represses genes that function in lymphocyte differentiation, inflammation, and cell cycle control Immunity, 13 (2000), pp. 199–212

35. W. Ci, J.M. Polo, L. Cerchietti, R. Shaknovich, L. Wang, S.N. Yang, K. Ye, P. Farinha, D.E. Horsman, R.D. Gascoyne, O. Elemento, A. Melnick The BCL6 transcriptional program features repression of multiple oncogenes in primary B cells and is deregulated in DLBCL Blood, 113 (2009), pp. 5536–5548

36. T. Yamochi, Y. Kaneita, T. Akiyama, S. Mori, M. Moriyama Adenovirus-mediated high expression of BCL-6 in CV-1 cells induces apoptotic cell death accompanied by down-regulation of BCL-2 and BCL-X(L) Oncogene, 18 (1999), pp. 487–494

37. T.T. Tang, D. Dowbenko, A. Jackson, L. Toney, D.A. Lewin, A.L. Dent, L.A. Lasky The forkhead transcription factor AFX activates apoptosis by induction of the BCL-6 transcriptional repressor J. Biol. Chem., 277 (2002), pp. 14255–14265

38. T. Kurosu, T. Fukuda, T. Miki, O. Miura BCL6 overexpression prevents increase in reactive oxygen species and inhibits apoptosis induced by chemotherapeutic reagents in B-cell lymphoma cells Oncogene, 22 (2003), pp. 4459–4468

39. B.W. Baron, E. Hyjek, B. Gladstone, M.J. Thirman, J.M. Baron PDCD2, a protein whose expression is repressed by BCL6, induces apoptosis in human cells by activation of the caspase cascade Blood Cells Mol. Dis., 45 (2010), pp. 169–175

40. H. Niu, B.H. Ye, R. Dalla-Favera Antigen receptor signaling induces MAP kinase-mediated phosphorylation and degradation of the BCL-6 transcription factor Genes Dev., 12 (1998), pp. 1953–1961

41. R.T. Phan, R. Dalla-Favera The BCL6 proto-oncogene suppresses p53 expression in germinal-centre B cells Nature, 432 (2004), pp. 635–639

42. K.H. Vousden, X. Lu Live or let die: the cell's response to p53 Nat. Rev. Cancer, 2 (2002), pp. 594–604

43. J. Iqbal, T.C. Greiner, K. Patel, B.J. Dave, L. Smith, J. Ji, G. Wright, W.G. Sanger, D.L. Pickering, S. Jain, D.E. Horsman, Y. Shen, K. Fu, D.D. Weisenburger, C.P. Hans, E. Campo, R.D. Gascoyne, A. Rosenwald, E.S. Jaffe, J. Delabie, L. Rimsza, G. Ott, H.K. Muller-Hermelink, J.M. Connors, J.M. Vose, T. McKeithan, L.M. Staudt, W.C. Chan P. Leukemia/Lymphoma molecular profiling, distinctive patterns of BCL6 molecular alterations and their functional consequences in different subgroups of diffuse large B-cell lymphoma Leukemia, 21 (2007), pp. 2332–2343

44. K. Boggs, D. Reisman Increased p53 transcription prior to DNA synthesis is regulated through a novel regulatory element within the p53 promoter Oncogene, 25 (2006), pp. 555–565

45. S.M. Oh, C.W. Pyo, Y. Kim, S.Y. Choi Neutrophil lactoferrin upregulates the human p53 gene through induction of NF-kappaB activation cascade Oncogene, 23 (2004), pp. 8282–8291

46. Shvarts, T.R. Brummelkamp, F. Scheeren, E. Koh, G.Q. Daley, H. Spits, R. Bernards A senescence rescue screen identifies BCL6 as an inhibitor of anti-proliferative p19(ARF)-p53 signaling Genes Dev., 16 (2002), pp. 681–686

47. S.M. Ranuncolo, L. Wang, J.M. Polo, T. Dell'Oso, J. Dierov, T.J. Gaymes, F. Rassool, M. Carroll, A. Melnick BCL6-mediated attenuation of DNA damage sensing triggers growth arrest and senescence through a p53-dependent pathway in a cell context-dependent manner J. Biol. Chem., 283 (2008), pp. 22565–22572

48. K. Vaiphei, N. Kumari, S.K. Sinha, U. Dutta, B. Nagi, K. Joshi, K. Singh Roles of syndecan-1, bcl6 and p53 in diagnosis and prognostication of immunoproliferative small intestinal disease World J. Gastroenterology: WJG, 12 (2006), pp. 3602–3608

49. E.W. Newcomb P53 gene mutations in lymphoid diseases and their possible relevance to drug resistance Leukemia Lymphoma, 17 (1995), pp. 211–221

50. O. Margalit, H. Amram, N. Amariglio, A.J. Simon, S. Shaklai, G. Granot, N. Minsky, A. Shimoni, A. Harmelin, D. Givol, M. Shohat, M. Oren, G. Rechavi BCL6 is regulated by p53 through a response element frequently disrupted in B-cell non-Hodgkin lymphoma Blood, 107 (2006), pp. 1599–1607

51. I.C. MacLennan Germinal centers Annu. Rev. Immunol., 12 (1994), pp. 117–139

52. K. Rajewsky Clonal selection and learning in the antibody system Nature, 381 (1996), pp. 751–758

53. U. Vitolo, B. Botto, D. Capello, D. Vivenza, V. Zagonel, A. Gloghini, D. Novero, G. Parvis, R. Calvi, C. Ariatti, I. Milan, M. Bertini, C. Boccomini, R. Freilone, P. Pregno, L. Orsucci, G. Palestro, G. Saglio, A. Carbone, E. Gallo, G. Gaidano Point mutations of the BCL-6 gene: clinical and prognostic correlation in B-diffuse large cell lymphoma Leukemia, 16 (2002), pp. 268–275

54. M.J. Artiga, A.I. Saez, C. Romero, M. Sanchez-Beato, M.S. Mateo, C. Navas, M. Mollejo, M.A. Piris A short mutational hot spot in the first intron of BCL-6 is associated with increased BCL-6 expression and with longer overall survival in large B-cell lymphomas Am. J. Pathol., 160 (2002), pp. 1371–1380

Corresponding author. Address: Department of Basic Medical Sciences, Neurosciences, and Sensory Organs, University of Bari Medical School, Piazza Giulio Cesare, 11 Policlinico, I-70124 Bari, Italy. Tel.: +39 0039 080 5478240; fax: +39 0039 080 5478310.

.